COMPARISON OF *GEANT4* WITH *EGSnrc* FOR SIMULATION OF GAMMA-RADIATION DETECTORS BASED ON SEMI-INSULATING MATERIALS

A.I. Skrypnyk**, *A.A. Zakharchenko, *M.A. Khazhmuradov

National Science Center "Kharkov Institute of Physics and Technology", 61108, Kharkov, Ukraine

(Received August 1 , 2011)

We considered *GEANT4* version 4.9.4 with different Electromagnetic Physics Package for calculation of response functions of detectors based on semi-insulating materials. Computer simulations with *GEANT4* packages were run in order to determine the energy deposition of gamma-quanta in detectors of specified composition (HgI_2 and TlBr) at various energies from 0.026 to 3 MeV. The uncertainty in these predictions is estimated by comparison of their results with *EGSnrc* simulations. A general good agreement is found for *EGSnrc* and *GEANT4* with *Penelope* 2008 model of LowEnergy Electromagnetic package.

PACS: 29.40.Wk, 85.30De

1. INTRODUCTION

The variety of electrophysical characteristics (specific resistance, product of mobility μ and mean drift time τ for holes and electrons – $(\mu\tau)_{h,e}$) is a serious disadvantage of semi-insulating materials (wide band-gap semiconductor with high resistivity). Now this is a main cause that the semi-insulator gamma-radiation detectors could not be mass produced. Wide band-gap semiconductor detectors have considerable spread of $(\mu\tau)_{h,e}$ values (in order of magnitude and more) [1] even if they are produced from one ingot. As result the same size detectors biased to the same voltage U_b have a different charge collection efficiency (*CCE*). It results in non-uniformity of serial devices response and in necessity of individual setup parameters selection.

Also the material non-uniformities are a serious obstacle to comparison of detector characteristics measured in different studies. Computer simulation is an optimal method to overcome the material non-uniformity problem. Simulation may be useful both to research of wide band-gap detector behavior and designing of device based on them [2].

Previously we have developed the model of the planar wide band-gap semiconducting gamma-radiation detectors where EGSnrc Monte-Carlo (MC) simulation package was used for determination of the energy deposition of gamma-quanta and charged particles [3]. This model was tested on the several groups of $CdTe$ and $CdZnTe$ detectors [4]. The observed difference between model and experimentally measured amplitude distributions of radiation sources ^{137}Cs and ^{152}Eu was explained in process of this model verification [2]. However, by this now all factors defining such important gamma-radiation detector characteristics as sensitivity δ and charge collection efficiency *CCE* are not determined even for the most researched semi-insulating materials as $CdTe$ and $CdZnTe$. By-turn it does not permit to define exhaustive set of the control parameters of the wide band-gap detector model. The determination of these parameters would allow calculating the most realistic response of the gamma-radiation detector.

The model [4] enabled to obtain a good agreement between calculated and experimental response functions of $CdTe$ ($CdZnTe$) gamma-radiation detectors in the most cases analyzed. However *EGSnrc* package possibilities are restricted only by a simulation of photon, electron and positron transport. It does not allow using the above mentioned model [4] for analysis of the charge collection efficiency experiments with the wide band-gap detectors when proton and α-particle beams are used [5]. Also the model [4] is unsuitable for researching of actual problems of radiation resistance of semi-insulators in mixed radiation fields (charged particles and/or neutrons and gamma-quanta) [6].

*Geant*4 [7] is an actively developing toolkit for the simulation of the passage of charged particles, neutrons and gamma-quanta through matter. This MC package offers a set of physical process models to describe the interaction of charged and neutral particles with matter in the wide energy range. *Geant*4 provides various models of the same electromagnetic processes (EM packages) [8]. To implement the model [4] on *Geant*4 platform properly it is necessary to define EM package which provides better agreement with *EGSnrc* simulation results.

In the present work statistical characteristics of

*Corresponding author E-mail address: belkas@kipt.kharkov.ua

the *EGSnrc*-calculated response functions of planar wide band-gap detectors based on HgI_2 and TlBr to gamma-quanta with energies between 0.026 and 3 MeV is compared with the results of *Geant*4 simulation. The same radiation source and detector geometry parameters are used to calculate the photon and charged particle transport in *EGSnrc* and *Geant*4 simulations. A good agreement between results of *EGSnrc* and *Geant*4 simulations is obtained with using *Penelope*-2008 EM package *Geant*4 v.4.9.4 [9].

2. THE *GEANT*4 AND *EGSnrc* ELECTROMAGNETIC MODELS

*Geant*4 includes three EM packages, which use different models for cross-sections of photons and charged particles interactions with the matter and different models for final state sampling algorithms. These are Standard EM model and two models for low energy region identified as *Livermore* and *Penelope* EM model. All models describe the photoelectric effect, the Compton scattering and the gamma conversion. The model processes of the induced emission and scattering e^-–e^- and e^-–e^+ are available for electrons and positrons.

In the recent years many articles were published where *Geant*4 simulation results are compared with yield of ≪reference≫ MC codes *EGSnrc* and *MCNP* [7–10]. *EGSnrc* and *MCNP* packages have longer application history in radiation physics and nuclear medicine in comparison with Geant4. As a result of often modifications of *Geant*4 code and fixation of algorithm bugs the comparison of different *Geant*4 version simulations with other Monte-Carlo codes and experimental data can show the differing results. In the present work *Geant*4 v.4.9.3 and v.4.9.4 simulations are compared with results of *EGSnrc* version 4r2.3.1.

The Standard model uses an analytical approach to describe the electromagnetic interactions in the range from 1 keV up to about 100 TeV. An analytical approach combines numerical databases with analytical cross-section models assuming quasi-free atomic electrons while the atomic nucleus is fixed. Transport of X- and gamma rays takes into account Compton scattering using the free-electron approximation, gamma conversion into electron-positron pair, and photoelectric effect. Bremsstrahlung and ionization are the available processes for electrons and positrons. The binding energy of atomic electrons is taken into account only at the photoelectric effect simulation. The simplified computational algorithm of the nuclear radiation transport through the matter provides the most calculating efficiency for the Standard model in comparison with other models. However, coherent (Rayleigh) scattering and atomic relaxation processes are not included for this package.

Atomic and shell ionization effects are included in the *Livermore* model. The lower energy threshold of the simulation interactions is decreased down to 250 eV. The available physical processes are Rayleigh and Compton scattering, photo-electric effect, pair production, bremsstrahlung, and ionization. The fluorescence and Auger emission in excited atoms are also considered. This package describes the electromagnetic interactions of electrons and photons taking into account subshell integrated cross sections for photoelectric effect, ionization, and electron binding energies for all subshells. Cross-sections of particle interactions with matter are calculated from evaluated data libraries from Lawrence Livermore National Laboratory – EPDL97 for photons [11], EEDL for electrons [12] and EADL for fluorescence and Auger effects [13].

The physical model which originally was developed for *Penelope* MC code [9] combines analytical approach for computation of cross-section of the different interactions with data from cross-section databases calculated in Seltzer and Berger work [14]. Algorithm *Penelope* 2008 is used in *Geant*4 beginning with version v.4.9.3. This model is applicable to interactions in range from about 200 eV up to 1 GeV. Now *Penelope* EM Package is still tested.

NIST data [14, 15] with empirical correction factors for set of elements [16] are employed for computation of bremsstrahlung loss in the *EGSnrc* model of the electromagnetic interactions. Cross-sections of the photoelectric effect, pair and triplet generation and coherent scattering cross-sections are determined from EDPL [11] and XCOM [17] estimations. The Klein-Nishina method allowing for Doppler broadening correction and correction for chemical bond effects is used to calculate the incoherent (Compton) scattering cross-sections. Parameters of atom relaxation are determined for every atomic subshell.

Contribution of the atom relaxation processes can be appreciable during registration of gamma-quanta with energies up to about 1 MeV. They are not described in the *Geant*4 Standard Electromagnetic Model. Thus it is possible to expect the largest difference between simulation data received with using Standard EM Package and *EGSnrc* simulation results.

3. RESULTS OF SIMULATIONS

Functions of gamma-quantum energy loss distribution (response functions) were computed for planar detectors based on two wide band-gap semiconducting compounds: mercuric (II) iodide (HgI_2) and thallium bromide (TlBr). HgI_2 detectors are investigated over a long period of time [18] while TlBr is a comparatively new material for nuclear radiation detection [19]. Initial energy of gamma-quantum beam was chosen in the range from 0.026 up to 3 MeV. Simulations were run for all three *Geant*4 packages of electromagnetic interactions. Geometric sizes of detectors and gamma-quantum beam parameters were identical for all *Geant*4 and *EGSnrc* models.

Since the thickness of investigated detectors was about 1 mm the minimal run length of *Geant*4-

simulated particles (*cutForElectron*) and gamma-quanta (*cutForGamma*) in detector material was set equal to 0.01 mm. It corresponds to the minimal energy 3.21 keV for gamma-quanta and 43.23 keV for electrons in HgI_2. The minimal energy of *Geant*4-simulated gamma-quanta in TlBr is 3.85 keV and 48.14 keV for electrons. The similar energy thresholds $PCUT = 2$ keV (gamma-quanta) and $ECUT = 20$ keV (electrons) were set for both materials during *EGSnrc* simulations.

In the present work we do not consider the energy loss of fast electrons due to the excitation of lattice vibrations. Statistical moments: average energy loss, variance and asymmetry coefficient were computed for every function of distribution of energy loss. Received dependences of the statistical moments against initial energy of gamma-quantum beam allow revealing and describing in detail systematical differences between results of *Geant*4 and *EGSnrc* simulation.

3.1 Mercuric (II) Iodide

Mercuric (II) iodine (HgI_2) belongs to the group of $A^{II}B^{VI}$ semiconductor compounds. The functions of distribution of gamma-quantum energy loss were computed for the planar HgI_2 detector with size of $5\times5\times1$ mm^3. The parallel monoenergetic gamma-quantum beam was uniformly scanned on the detector area. The beam incidence angle was equal to 90°. At the first stage of the pesent work we used *Geant*4 v.4.9.3-p01 for comparison with *EGSnrc* simulations. 10^6 gamma-quantum histories were simulated for every energy. The statistical moments of the response functions were calculated on their base.

Fig. 1 shows the dependence of average energy losses $<E>$ of gamma-quanta (the first moment) against initial beam energy in the investigated HgI_2 detector. Calculated energy losses are practically equal for all investigated models in the energy range less than $E_\gamma < 0.4$ MeV. The energy losses calculated from Standard and Livermore simulation data are stably lower than results of EGSnrc simulations in region $E_\gamma > 0.4$ MeV.

The predicted mean energy losses of gamma-quanta received from Standard and *Livermore* models practically coincides in the range between 0.4 and 2 MeV. But the Geant4 v.4.9.3-p01 simulation demonstrates abrupt increase of the mean losses for *Livermore* model relative to Standard model data for gamma-quantum energies above $E_\gamma > 2$ MeV (Fig. 1). The quick increase of the electron-positron pair production cross-section is a single essential feature of the gamma-quantum interaction with HgI_2 in energy range above $E_\gamma > 2$ MeV. Consequently observed difference (Fig. 1) may be concerned with *Geant*4 v.4.9.3-p01 errors of the positron trajectory simulation.

The repeated simulation of the HgI_2-detector response functions using *Geant*4 v.4.9.4-p02 (release from 24-06-2011) showed that these bugs have been fixed by authors. Moreover, as Fig. 1 shows the difference between *Penelope* model data in version 4.9.4-p02 and result of *EGSnrc* simulation considerably decreased. That is why, except where noted, for further study we use results received from *Geant*4 v.4.9.4-p02 simulations.

To reveal the most essential differences between simulation results received with different *Geant*4 EM packages it is necessary the detailed analysis of the investigated HgI_2-detector response functions in the energy range of gamma-quanta where different physical processes are dominated.

Fig. 2 shows the computed distributions of gamma-quantum energy losses for initial beam energy $E_\gamma = 0.08$ MeV. At this energy the photoelectric effect is a dominating process of the gamma-radiation interaction with HgI_2. The amount of absorbed photons (on the Fig. 2 and further these events correspond to energy E_γ) for all models insignificantly differs (Table 1). It confirms that similar values of photoelectric effect cross-sections for Hg and I are used in all models. Atomic relaxation processes are not taken into account in the Standard model. Therefore the photoelectric effect event quantity is maximal for this model.

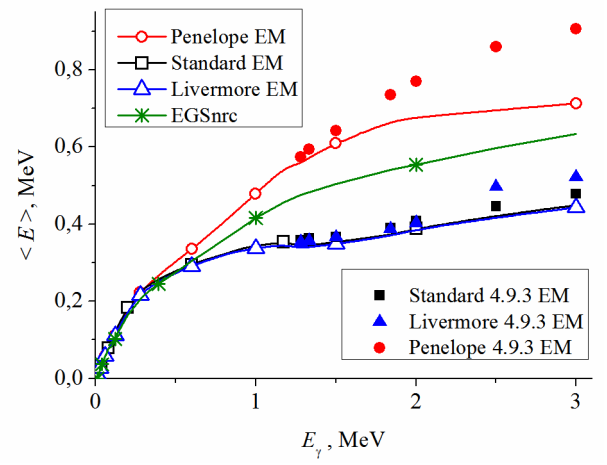

Fig.1. *The dependence of average energy losses of gamma-quanta in HgI_2 vs initial beam energy*

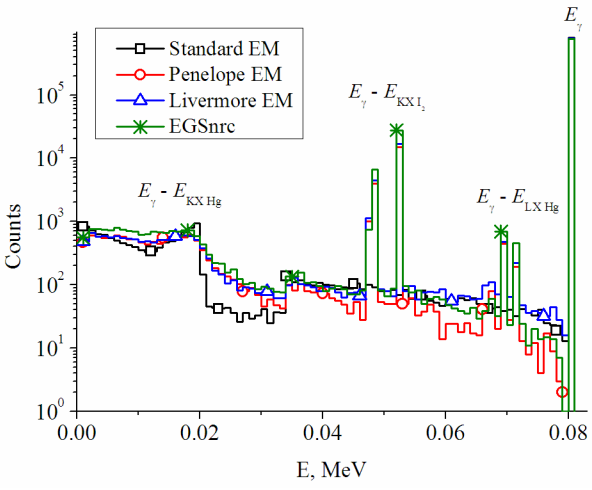

Fig.2. *Energy losses of gamma-quanta with energy $E_\gamma = 0.08$ MeV in HgI_2-detector*

Table 1 and follow-up data show that the total efficiency of registration of gamma-quanta of investigated detectors is almost the same for all models.

The fine structure of escape peaks is reconstructed from the results of *EGSnrc* simulations in the most detail. As Fig. 2 demonstrates the used energy bin (1 keV) allows separating *KX*- and *LX*-series of characteristic photons for both elements (Hg and I).

Table 1. *The amount of photoelectric effect events and total efficiency for gamma-quanta with* $E_\gamma = 0.08$ *MeV*

EM model	Photoeffect	Efficiency, HgI_2
Standard	804176	0.818
Livermore	784069	0.822
Penelope	788043	0.822
EGSnrc	765231	0.819

In low-loss energy region of HgI_2-detector response functions computed with using *Livermore* and *Penelope* EM models show good agreement with *EGSnrc* simulation data. According to Fig. 2 these three models have an almost equal distribution of the energy losses in the region up to 0.04...0.045 MeV. In the energy loss region above 0.045 MeV the better agreement with *EGSnrc* data is observed for *Livermore* EM model.

All EM models lead to the similar distribution of the Compton tail in the gamma-quantum energy region where Compton scattering is prevailed (Fig. 3). Computations with *Penelope* EM model allow obtaining the better agreement with *EGSnrc* simulation in the Compton valley whereas Standard and *Livermore* results exceed *EGSnrc* data. At the same time the amount of absorbed gamma-quanta for the *Livermore* model is equal about two thirds of the same as other models (Table 2).

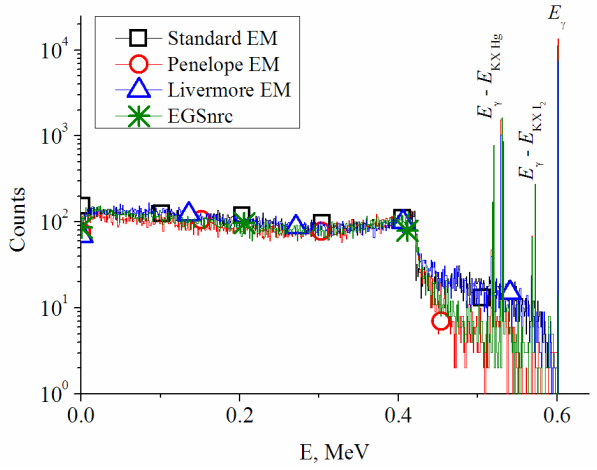

Fig.3. *Energy losses of gamma-quanta with energy* $E_\gamma = 0.6$ *MeV in* HgI_2*-detector*

As follows Fig. 4 and Table 3 data the *Livermore* and Standard EM models employ cross-sections of photoelectric interaction with HgI_2 for gamma-quanta with energy $E_\gamma = 1.28$ MeV which values are much less compared with the same in the *Penelope* EM model and *EGSnrc*. It is confirmed by the lack of photopeaks for the response functions simulated with using these models. Moreover the disappearing of the Compton edges on the Fig. 4 indicates that the *Livermore* and Standard models employ smaller probabilities of the gamma-quantum Compton scattering angels above 135° in comparison with the *Penelope* model and *EGSnrc*.

Table 2. *The amount of photoelectric effect events and total efficiency for gamma-quanta with* $E_\gamma = 0.6$ *MeV*

EM model	Photoeffect	Efficiency, HgI_2
Standard	12602	0.058
Livermore	7418	0.057
Penelope	13488	0.058
EGSnrc	11312	0.058

If gamma-quantum energy is enough for electron-positron pair production (gamma-conversion) (for example $E_\gamma = 1.28$ MeV, Fig. 4) a double-escape peak of annihilation gamma-quanta becomes appreciable in the Geant4 simulations (Table 3). On the Fig. 4 these events correspond to the energy equal to 0.259 MeV. According to *EGSnrc* simulation of response function of investigated HgI_2-detector at energy $E_\gamma = 1.28$ MeV the double escape peak is not yet observed (Table 3).

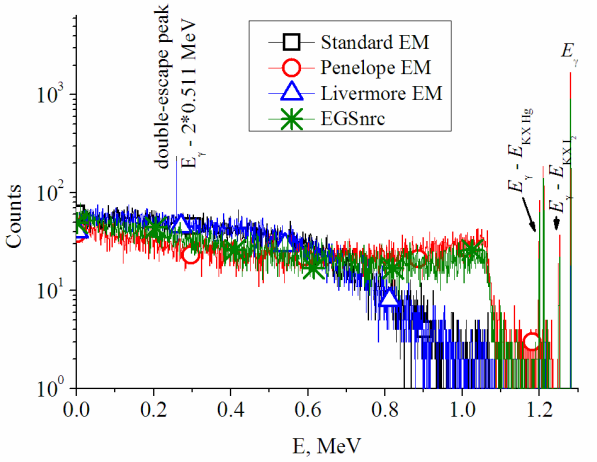

Fig.4. *Energy losses of gamma-quanta with energy* $E_\gamma = 1.28$ *MeV in* HgI_2*-detector*

Table 3. *The amount of the photoelectric effect and double escape events for gamma-quanta with* $E_\gamma = 1.28$ *MeV* (HgI_2)

EM model	Photoeffect	Double-escape
Standard	39	234
Livermore	18	209
Penelope	1700	201
EGSnrc	1083	37

Above results show that there is good agreement between the response functions of the investigated HgI_2-detector received with the *Penelope* and *EGSnrc* model apart from double-escape peak of the annihilation gamma-quanta.

Finally, the computation of the HgI_2-detector response function based on the 10^7 simulation trajectories of gamma-quanta with energy $E_\gamma = 3$ MeV shows a good agreement between results of the *Penelope* EM model and *EGSnrc* (Fig. 5). Plots corresponding to results of the *Livermore* and Standard models are located appreciably lower. The escape peaks in that models are absent (Table 4 and Fig. 5). This indicates that values of cross-section of the electron-positron pair production employed by the *Livermore* and Standard models are smaller as compared with the same of the *Penelope* EM model and *EGSnrc*.

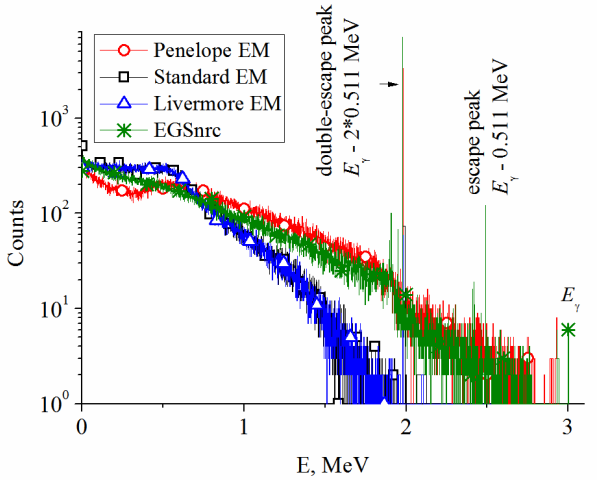

Fig.5. *Energy losses of gamma-quanta with energy $E_\gamma = 3$ MeV in HgI_2-detector*

Table 4. *The amount of event of the escape and double escape of annihilation gamma-quanta (HgI_2), $E_\gamma = 3$ MeV*

EM model	Escape	Double-escape
Standard	1	74
Livermore	0	59
Penelope	65	3366
EGSnrc	121	7152

Fig. 5 shows that the response functions of the HgI_2-detector received with the *Geant*4 v4.9.4-p02 *Livermore* and Standard models practically coincide. So average energy losses of gamma-quanta with energy 3 MeV also coincide (Fig. 1). It confirms our supposition about the incorrect computation of the HgI_2-detector response functions when *Geant*4 v.4.9.3-p01 *Livermore* and Standard models have been used (Fig. 1).

Other statistical characteristics of response functions of the investigated HgI_2-detector – variance (Fig. 6) and skewness coefficient (Fig. 7) – also demonstrate a good agreement between results of *Geant*4 v4.9.4-p02 *Penelope* EM package simulations and *EGSnrc* data.

From Fig. 1, Fig. 6 and Fig. 7 it follows that main differences of all statistical characteristics of the HgI_2-detector response functions between *Geant*4 v4.9.3-p01 and v4.9.4-p02 simulation data correspond to the electron-positron pair production region (E_γ > 1.022 MeV). In the gamma-quantum energy region where positrons are not generated the response functions received with different Geant4 versions coincide. Therefore the cause of anomalous simulation results is incorrect values of specific ionization energy losses of positrons in HgI_2 those used by *Geant*4 v4.9.3-p01. The differences between response functions of the investigated TlBr-detector received using of both *Geant*4 versions are insignificant.

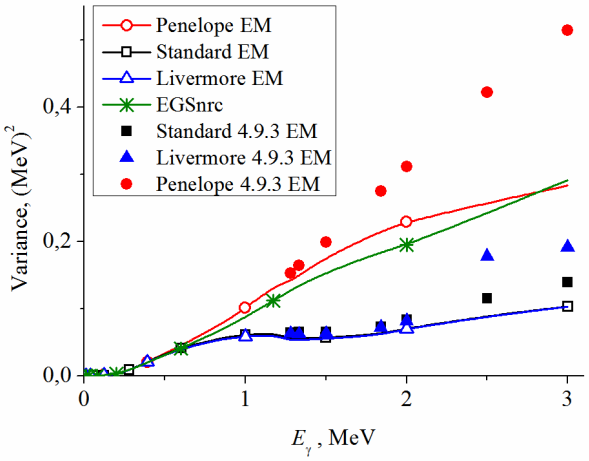

Fig.6. *The dependence of variance of the HgI_2-detector response functions vs gamma-quantum energy*

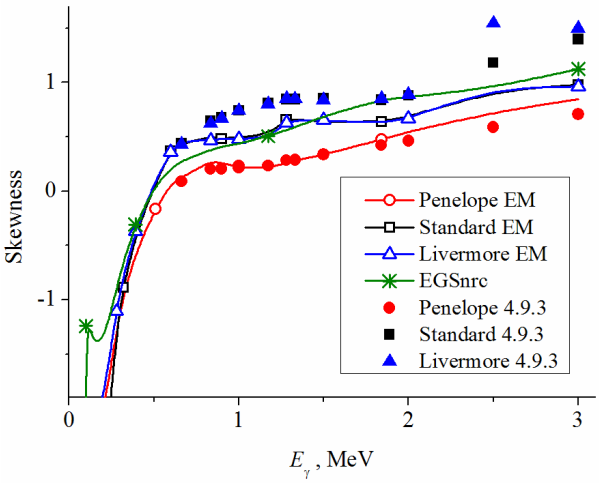

Fig.7. *The dependence of skewness coefficient of the HgI_2-detector response functions vs gamma-quantum energy*

3.2 Thallium Bromide

Thallium bromide (TlBr) belongs to the group of $A^{III}B^{VI}$ semiconductor compounds. Quality differences between the linear gamma-ray attenuation coefficients of TlBr and HgI_2 are negligible. These differences are characteristic for the energy region where photoelectric effect is dominated (Fig. 8). At the same time the TlBr linear gamma-ray attenuation coefficient exceeds the same of HgI_2 about 10% beginning from gamma-ray energy $E_\gamma = 0.1$ MeV. As follows we can expect that average losses of gamma-quanta energy in TlBr will be higher than in HgI_2 at

the same detector thickness.

Distributions of the gamma-quantum energy losses were calculated for the planar TlBr-detector with size of 3.142 mm^2 × 0.8 mm. The parallel monoenergetic beam of gamma-quanta was uniformly distributed on the detector area. The beam incidence angle was equal to 90°. 10^6 histories were simulated for each gamma-ray energy. Statistical moments of response functions were calculated using these histories (Fig. 9 and Fig. 10).

The data plotted on the Fig. 9 – Fig. 12 are received from the *Geant*4 v4.9.4-p02 simulations. Response functions of the investigated TlBr-detector obtained using version v.4.9.3 coincide with version v.4.9.4 calculations within the scope of statistical uncertainties. It gives grounds for affirmation that the reason of above-mentioned anomalous simulation results for HgI_2-detector is not the errors of the positron trajectory simulation algorithm. As we think these anomalous results are consequence of incorrect values of the specific ionization energy losses of positrons in HgI_2. Similarly the case of HgI_2-detector the better coincidence between *EGSnrc* and *Geant*4 simulation data is observed when the *Penelope* model of electromagnetic interactions has been used (Fig. 9 and Fig. 10).

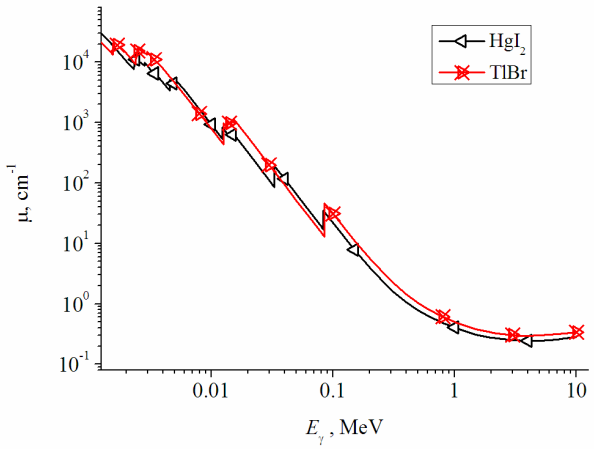

Fig.8. *The linear gamma-ray attenuation coefficient for HgI_2 and TlBr [17]*

The analysis of simulated TlBr-detector response functions for gamma-ray photons with energy E_γ = 0.6 MeV (Fig. 11) shows the presence of escape peaks of characteristic photons of Tl and Br KX-series in all models apart from the Standard EM model. The Compton tail is identically reconstructed in all simulations. As for the Compton valley region that the better agreement with *EGSnrc* data is obtained for the *Geant*4 *Penelope* EM package simulation. The amount of the absorbed gamma-quanta with the energy 0.6 MeV for the *Livermore* EM model simulation is about 30% less in comparison with other models (Table 5).

The response function of the investigated TlBr-detector for rather high energy gamma-quanta (E_γ = 3 MeV, Fig. 12) received with using *EGSnrc* MC package shows a good agreement only with the results of the *Geant*4 *Penelope* model simulation. For the *Livermore* and Standard models the escape peak of the annihilation gamma-quanta is almost absent and amplitude of the double escape peak is more than an order of magnitude less as compared with other simulations (Table 6).

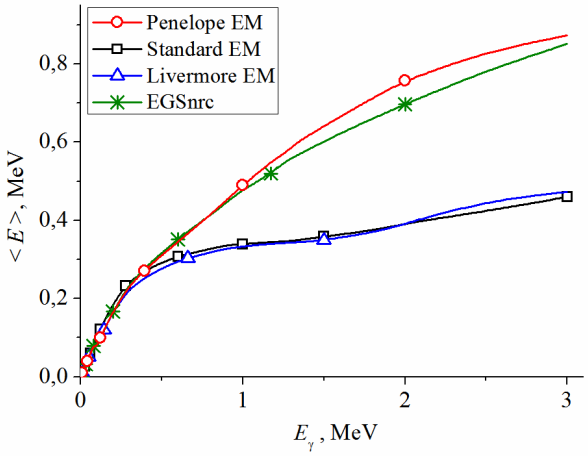

Fig.9. *The dependence of average energy losses of gamma-quanta in TlBr vs the initial energy beam*

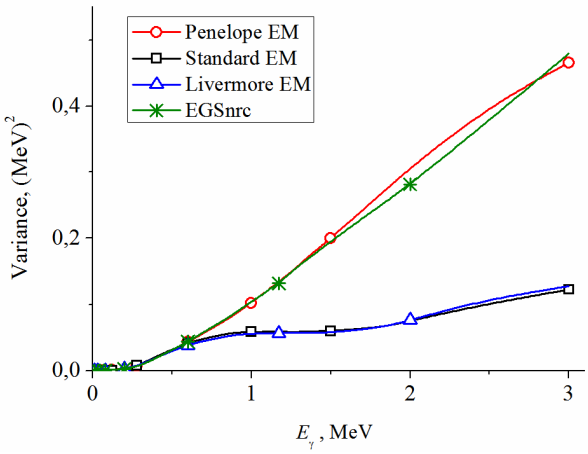

Fig.10. *The dependence of variance of TlBr-detector response functions vs the gamma-quantum energy*

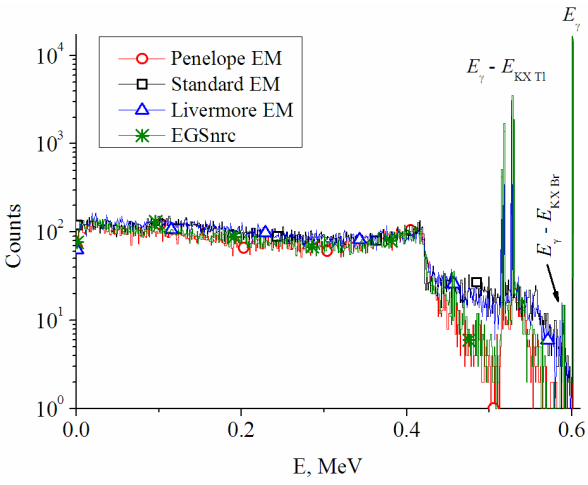

Fig.11. *The energy losses of gamma-quanta with the energy E_γ = 0.6 MeV in TlBr-detector*

Table 5. *The amount of photoelectric effect events and total efficiency for gamma-quanta with* $E_\gamma = 0.6$ *MeV*

EM model	Photoeffect	Efficiency, TlBr
Standard	14288	0.061
Livermore	9231	0.060
Penelope	15652	0.060
EGSnrc	16804	0.064

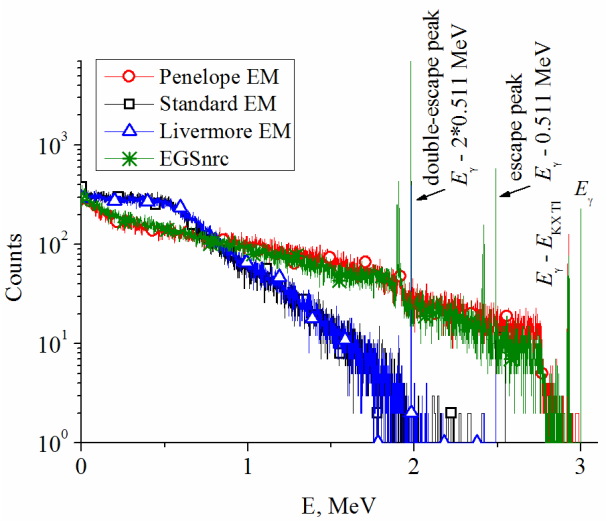

Fig.12. *The energy losses of gamma-quanta with the energy* $E_\gamma = 3$ *MeV in TlBr-detector*

Table 6. *The amount of event of the escape and double escape of annihilation gamma-quanta (TlBr),* $E_\gamma = 3$ *MeV*

EM model	Escape	Double-escape
Standard	13	435
Livermore	5	395
Penelope	235	5881
EGSnrc	577	13433

4. CONCLUSIONS

The comparison of the response functions of the HgI_2 and TlBr gamma-radiation detectors computed for all models of the electromagnetic interactions of the *Geant*4 package and *EGSnrc* has been made in this work. In the energy region of gamma-quanta up to 0.4 MeV there is a good agreement between response functions of the investigated detectors calculated with using *EGSnrc* and both *Livermore* and *Penelope* models of the *Geant*4 package. For wider gamma-quantum energy region between 0.026 and 3 MeV statistical parameters of the response functions simulated with *EGSnrc* and *Geant*4 packages have a good agreement only when the *Penelope* model of electromagnetic interactions has been used.

By the HgI_2-detector example it is shown that the comparison of the response functions received with using different simulation packages allow removing incorrect results and explaining the reason of their appearance.

References

1. G. Sato, A. Parsons, D. Hullinger et al. Development of a spectral model based on charge transport for the Swift/BAT 32K CdZnTe detector array // *Nucl. Instr. and Meth. A.* 2005, v. 541, p. 372–384.

2. A.A. Zakharchenko, M.A. Khazhmuradov. *Investigation of the properties of semiconductor detectors of nuclear radiation by the Monte Carlo method. Part 1: Semiconductor detectors of gamma radiation.* Preprint. NASU, NSC KIPT: Review, 2011, 1-48 (in Russian).

3. I. Kawrakow, E. Mainegra-Hing, D. Rogers. EGSnrcMP, the new multi-platform version of EGSnrc // *Med. Phys.* 2004, v. 31, p. 1731.

4. A.A. Zakharchenko, A.A. Veryovkin, V.E. Kutny, A.V. Rybka, M.A. Khazhmuradov. Simulation of response function of CdZnTe detectors for gamma-radiation dosimetry // *The Journal of Kharkov National University, Physical series: Nuclei, Particles, Fields.* 2008, no 832, issue 4(40), p. 71–76. (in Russian).

5. M. Breese, E. Vittone, G. Vizkelethy, P. Sellin. A review of ion beam induced charge microscopy // *Nucl. Instr. and Meth. B.* 2007, v. 264, p. 345–360.

6. A. Cavallini, B. Fraboni, W. Dusi et al. Radiation effects on II–VI compound-based detectors // *Nucl. Instr. and Meth. A.* 2002, v. 476, p. 770–778.

7. K. Amako, S. Guatelli, V. Ivanchencko et al. Geant4 and its validation // *Nuclear Physics B (Proc. Suppl.)* 2006, v. 150, p. 44–49.

8. G. Cirrone, G. Cuttone, F. Di Rosa et al. Validation of the Geant4 electromagnetic photon cross-sections for elements and compounds // *Nucl. Instr. and Meth. A.* 2010, v. 618, p. 315–322.

9. J. Sempau, J. Fernandez-Varea, E. Acosta, F. Salvat. Experimental benchmarks of the Monte-Carlo code PENELOPE // *Nucl. Instr. and Meth. B.* 2003, v. 207, p. 107-123.

10. H. Yoriyaz, M. Moralles, P. Siqueira et al. Physical models, cross sections, and numerical approximations used in MCNP and GEANT4 Monte Carlo codes for photon and electron absorbed fraction calculation // *Med. Phys.* 2009, v. 36 (11), p. 5198-5213.

11. D. Cullen, J. Hubbell, L. Kissel. *EPDL97: The Evaluated Photon Data Library '97 Version* LLNL: UCRL-50400, vol. 6, rev. 5, 1997; http://www-nds.iaea.org/epdl97/document/epdl97.pdf

12. S. Perkins, D. Cullen, S. Seltzer. *Tables and graphs of electron-interaction cross-sections from 10 eV to 100 GeV derived from the LLNL evaluated electron data library (EEDL), Z=1–100* LLNL: Report UCRL-50400, vol. 31, 1991.

13. S. Perkins, M. Chen, D. Cullen et al. *Tables and graphs of atomic subshell and relaxation data derived from the LLNL evaluated atomic data library (EADL), Z=1–100.* LLNL: Report UCRL-50400, vol. 30, 1992.

14. S. Seltzer and M. Berger. Bremsstrahlung Spectra from Electron Interactions with Screened Atomic Nuclei and Orbital Electrons // *Nucl. Instr. and Meth. B.* 1985, v. 12, p. 95–134.

15. S. Seltzer and M. Berger. Bremmstrahlung Energy Spectra from Electrons with Kinetic Energy from 1 keV to 10 GeV Incident on Screened Nuclei and Orbital Electrons of Neutral Atoms with Z = 1-100 // *Atomic Data and Nuclear Data Tables.* 1986, v. 35, p. 345–418.

16. C. Myers, B. Kirk, L. Leal. Comparative analysis of nuclear cross sections in Monte Carlo methods for medical physics applications // Computational Medical Physics Working Group Workshop II, Sep 30 – Oct 3, 2007; http://cmpwg.ans.org/oct2007/Presentations/T203.pdf

17. XCOM: Photon Cross Sections Database, National Institute of Standards and Technology (1998); http://www.nist.gov/pml/data/xcom/index.cfm

18. H. Malm. A Mercuric Iodide Gamma-Ray Spectrometer // *IEEE Trans. Nucl. Sci.* 1972, v. 19, p. 263–265.

19. K. Hitomi, O. Muroi, T. Shoji et al. Room temperature X- and gamma-ray detectors using thallium bromide crystals // *Nucl. Instr. and Meth. A.* 1999, v. 436, p. 160–164.